JACS
JOURNAL OF THE AMERICAN CHEMICAL SOCIETY

Communication

pubs.acs.org/JACS

Discovery of Face-Centered-Cubic Ruthenium Nanoparticles: Facile Size-Controlled Synthesis Using the Chemical Reduction Method

Kohei Kusada,[†] Hirokazu Kobayashi,[†,‡] Tomokazu Yamamoto,[‡,∥] Syo Matsumura,[‡,∥] Naoya, Sumi,[‡,⊥] Katsutoshi Sato,[‡,⊥,¶] Katsutoshi Nagaoka,[‡,⊥] Yoshiki Kubota,[§] and Hiroshi Kitagawa*[,†,‡,#,▽]

[†]Division of Chemistry, Graduate School of Science, Kyoto University, Kitashirakawa Oiwake-cho, Sakyo-ku, Kyoto 606-8502, Japan

[‡]Core Research for Evolutional Science and Technology (CREST), Japan Science and Technology Agency (JST), 5 Sanban-cho, Chiyoda-ku, Tokyo 102-0075, Japan

[∥]Department of Applied Quantum Physics and Nuclear Engineering, Kyushu University, 744 Motooka, Nishi-ku, Fukuoka 819-0395, Japan

[⊥]Department of Applied Chemistry, Faculty of Engineering, Oita University, 700 Dannoharu, Oita 870-1192, Japan

[¶]Energy Technology Research Institute, National Institute of Advanced Industrial Science and Technology (AIST), 1-1-1 Umezono, Tsukuba, Ibaraki 305-8568, Japan

[§]Department of Physical Science, Graduate School of Science, Osaka Prefecture University, 1-1 Gakuen-cho, Naka-ku, Sakai, Osaka 599-8531, Japan

[#]Institute for Integrated Cell-Material Sciences (iCeMS), Kyoto University, Yoshida, Sakyo-ku, Kyoto 606-8501, Japan

[▽]INAMORI Frontier Research Center, Kyushu University, 744 Motooka, Nishi-ku, Fukuoka 819-3095, Japan

Supporting Information

ABSTRACT: We report the first discovery of pure face-centered-cubic (fcc) Ru nanoparticles. Although the fcc structure does not exist in the bulk Ru phase diagram, fcc Ru was obtained at room temperature because of the nanosize effect. We succeeded in separately synthesizing uniformly sized nanoparticles of both fcc and hcp Ru having diameters of 2−5.5 nm by simple chemical reduction methods with different metal precursors. The prepared fcc and hcp nanoparticles were both supported on γ-Al_2O_3, and their catalytic activities in CO oxidation were investigated and found to depend on their structure and size.

The majority of metals have one of the three basic structures: body-centered cubic (bcc), hexagonal close-packed (hcp) or face-centered cubic (fcc). In the periodic table, as the atomic number increases across the transition metal series, the well-known canonical hcp−bcc−hcp−fcc structural sequence occurs, and the relative stability of the structure is determined by the total electronic energy of the metal.[1] The pressure−temperature (P−T) phase diagrams for bulk metals have been extensively investigated,[2] but when the size is reduced to nanodimensions, the phase diagrams of metals change considerably from the bulk.[3] For example, fcc Co and fcc Fe nanoparticles are stabilized under ambient conditions, even though these phases exist in the bulk only at high temperature.[4]

Ru is a 4d transition metal that in the bulk adopts an hcp structure at all temperatures, and it has recently attracted much attention as a catalyst for CO oxidation because of its high catalytic activity.[5] CO oxidation catalysts have been extensively investigated because of their potential applications in removal of CO from car exhausts and preventing CO poisoning in fuel-cell systems.[6] Moreover, steam reforming of shale gas is a popular source of synthetic gas for the generation of various chemical products and is strongly expected to be an important energy source in the near future. Recently, Ru has also attracted much attention as an effective catalyst for the steam-reforming reaction of methane which is the main component of shale gas.[7] Here we report the first example of fcc Ru and also demonstrate an easy synthesis method that allows the size of the nanoparticles to be controlled. The structure and size dependence of the catalytic activity of Ru nanoparticles in CO oxidation was observed.

Uniformly sized fcc and hcp Ru nanoparticles with sizes of 2−5.5 nm were prepared by chemical reduction methods using $Ru(acac)_3$ and $RuCl_3 \cdot nH_2O$, respectively, as the metal precursors and poly(*N*-vinyl-2-pyrrolidone) (PVP) as the stabilizing agent. Ethylene glycol (EG) or triethylene glycol (TEG) was employed as the solvent and reducing agent for the synthesis. Phase control was achieved by varying both the metal precursor and the solvent, and size control was achieved by adjusting the concentrations of the reagents and the PVP stabilizer used for the synthesis (Table 1). In a typical synthesis of fcc Ru nanoparticles having a diameter of 2.4 nm, $Ru(acac)_3$ (2.1 mmol) and PVP (10 mmol of monomer units) were dissolved in TEG (500 mL) at room temperature. The solution was then heated to 200 °C and maintained at this temperature for 3 h. After the reaction was complete, the prepared nanoparticles were separated by centrifugation. The syntheses of fcc and hcp Ru nanoparticles larger than 3.5 nm were performed using this method, but an adequate amount of PVP was added into the reaction solution after 3 h of heating to

Received: November 16, 2012
Published: April 4, 2013

Table 1. Reaction Conditions for the Synthesis of fcc and hcp Ru Nanoparticles

sample	structure	size (nm)	metal precursor/ mmol	solvent/ mL	mmol of PVP
A	fcc	2.4 ± 0.5	$Ru(acac)_3$/2.1	TEG/ 500	10.0
B	fcc	3.5 ± 0.7	$Ru(acac)_3$/2.1	TEG/ 200	10.0
C	fcc	3.9 ± 0.8	$Ru(acac)_3$/2.1	TEG/ 100	5.0
D	fcc	5.4 ± 1.1	$Ru(acac)_3$/2.1	TEG/25	1.0
E	hcp	2.2 ± 0.5	$RuCl_3{\cdot}nH_2O$/2.1	EG/500	10.0
F	hcp	3.5 ± 0.6	$RuCl_3{\cdot}nH_2O$/2.1	EG/200	10.0
G	hcp	3.9 ± 0.6	$RuCl_3{\cdot}nH_2O$/2.1	EG/100	5.0
H	hcp	5.0 ± 0.7	$RuCl_3{\cdot}nH_2O$/2.1	EG/25	1.0

adjust the relative amount of PVP to be similar to that for the smaller nanoparticles.

To investigate the size of the prepared samples, transmission electron microscopy (TEM) images were obtained with a Hitachi HT7700 TEM instrument operated at 100 kV. The TEM images in Figure 1show the formation of uniform Ru nanoparticles A–H having diameters of 2.2–5.4 nm with narrow size distributions. The mean diameters and distributions (Table 1) were estimated by averaging over >200 particles.

The crystal structure of the Ru nanoparticles was investigated by powder X-ray diffraction (PXRD) analysis using a Bruker D8 Advance diffractometer with Cu Kα radiation. Figure 2 shows

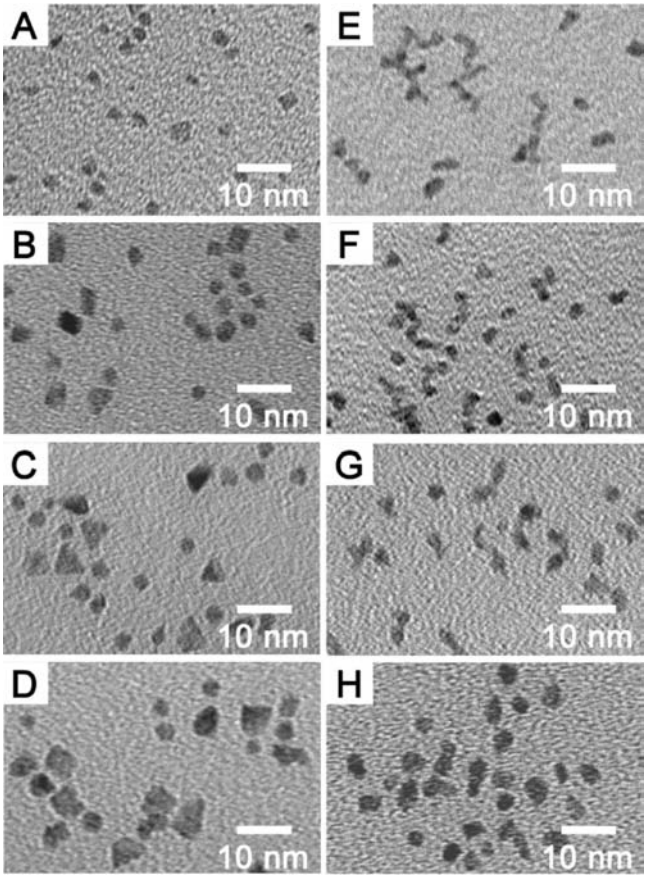

Figure 1. TEM images of synthesized (A–D) fcc and (E–H) hcp Ru nanoparticles with diameters of (A) 2.4, (B) 3.5, (C) 3.9, (D) 5.4, (E) 2.2, (F) 3.5, (G) 3.9, and (H) 5.0 nm.

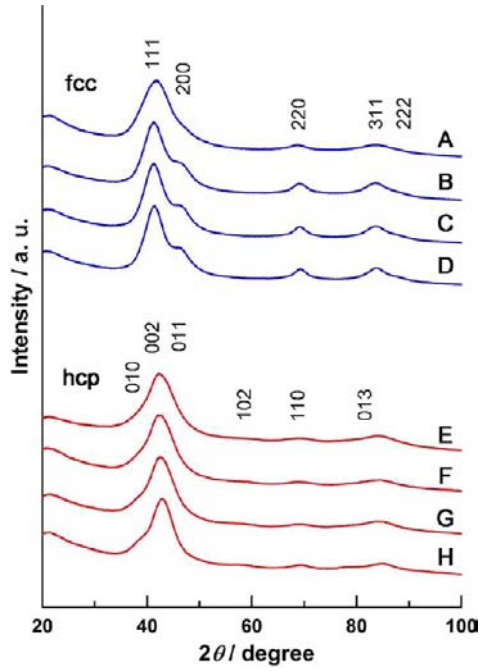

Figure 2. PXRD patterns for (A–D) fcc and (E–H) hcp Ru nanoparticles at room temperature. The radiation wavelength was 1.54 Å (Cu Kα).

the patterns for all of the prepared Ru nanoparticles. The trend in the XRD patterns correlated well with the TEM images, as the diffraction peaks became sharper as the mean particle size increased. One of the most noteworthy outcomes in this study is that the structure of the Ru nanoparticles could be controlled simply by choosing adequate combinations of the metal precursor and the reducing agent. All of the Ru nanoparticles synthesized with $Ru(acac)_3$ and TEG adopted an fcc structure, whereas those synthesized with $RuCl_3{\cdot}nH_2O$ and EG had an hcp structure. While several computational studies have reported the possibility of an fcc phase in Ru,[8] to the best of our knowledge, this is the first report of the synthesis of fcc Ru.

The structure of the prepared nanoparticles was also confirmed through selected-area electron diffraction (SAED) and high-resolution TEM (HRTEM) analysis using a JEOL JEM-ARM 200F microscope with spherical-aberration correctors (CEOS GmbH) operated at 200 kV. HRTEM images were recorded in the Gatan Ultrascan 1000 CCD camera without objective aperture. Images of fcc and hcp nanoparticles are presented in Figure 3. The image of an hcp Ru nanoparticle

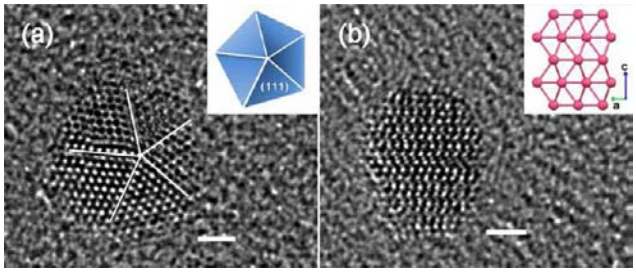

Figure 3. (a) HRTEM image of an fcc nanoparticle in sample D. The inset is an illustration of the decahedral structure. (b) HRTEM image of an hcp nanoparticle in sample H. The inset is an illustration of the hcp lattice viewed along the [100] direction. The scale bars are 1.0 nm.

dx.doi.org/10.1021/ja311261s | J. Am. Chem. Soc. 2013, 135, 5493–5496

recorded along the [100] direction (Figure 3b) clearly shows the hcp ABABAB... stacking sequence. On the other hand, Figure 3a shows a Ru nanoparticle representing the {111} fcc planes. This is a single fivefold-symmetry twinned nanoparticle having a decahedral structure consisting of five tetrahedrons. The decahedral structure is well-known as a typical structure of fcc metal nanoparticles such as Au, Ag, and Pd.[9] The details of the SAED and HRTEM analyses are described in Figures S1−S3 in the Supporting Information. These results confirmed that the crystal structure of Ru nanoparticles can be controlled by adjusting the synthetic precursor.

To investigate further the thermal stability of fcc Ru nanoparticles, we performed in situ PXRD measurements at the BL02B2 beamline at SPring-8 (Figure S4). The prepared Ru nanoparticles showed the fcc structure over a wide range of temperatures and were stable up to 723 K.

To investigate the catalytic activity of the synthesized nanoparticles in CO oxidation, the Ru nanoparticles were supported on γ-Al_2O_3 by the wet impregnation method. The catalysts were heated in increments of 10 °C to the temperature at which CO was consumed completely, and the products were analyzed at each temperature. The variation in CO conversion with temperature on Ru nanoparticles supported on γ-Al_2O_3 is summarized in Figure S5.

Figure 4 compares the CO conversions for 1 wt % loadings of each size of nanoparticle supported on γ-Al_2O_3. For the hcp

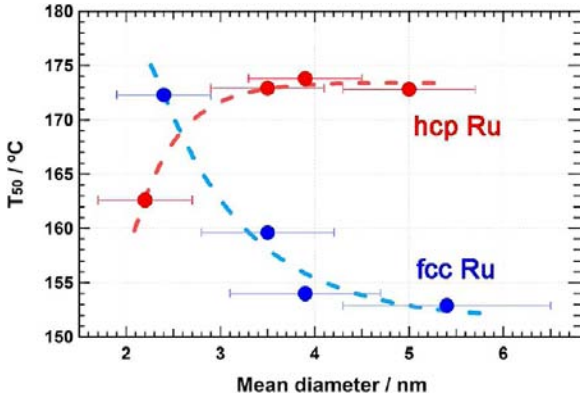

Figure 4. Size dependence of the temperature for 50% conversion of CO to CO_2 (T_{50}) for fcc (blue) and hcp (red) Ru nanoparticles.

Ru nanoparticles, the temperature for 50% conversion of CO to CO_2 (T_{50}) increased with particle size, a trend similar to that for Au or Rh nanoparticles.[10] Conversely, for the fcc Ru nanoparticles, T_{50} decreased with increasing particle size, similar to the trend observed for Pt nanoparticles.[11] Above 3 nm, the newly discovered fcc Ru nanoparticles were more reactive than the conventional hcp Ru nanoparticles. It has been reported that the mechanism of CO oxidation with hcp Ru begins with the oxidation of Ru(001) to form a few RuO_2(110) layers, after which the CO oxidation occurs on RuO_2(110).[12] The fcc (111) plane is also a close-packed plane in common with the hcp (001) plane. Although hcp nanoparticles are not completely enclosed by only close-packed planes, fcc nanoparticles generally tend to be enclosed by (111) planes because these planes have the lowest surface energy.[13] Therefore, the fcc Ru surface could be more reactive than that of hcp Ru for CO oxidation. In addition, the higher catalytic activity of the fcc Ru nanoparticles may be attributed in part to the presence of defects such as twin boundaries, fivefold symmetry axes, or distortion of the lattice parameter to fill space. However, the size dependences are different. This tendency might result from the differences in the formation process of oxide layers, the adsorption behavior of CO, or the activation energy, because of the differences in the electronic states and surfaces in the fcc and hcp structures. Further studies, including theoretical calculations, are required to understand the oxidation mechanism for fcc Ru.

In summary, we have reported the first synthesis of fcc Ru nanoparticles and the facile method for their synthesis. While hcp is the only phase in bulk Ru, the fcc phase was obtainable as a nanoparticulate phase. The structure of Ru nanoparticles can be controlled by choosing adequate combinations of the Ru precursor and reducing agent. All of the Ru nanoparticles synthesized with $Ru(acac)_3$ and triethylene glycol had the fcc structure, whereas the Ru nanoparticles synthesized with $RuCl_3 \cdot nH_2O$ and ethylene glycol had the hcp structure. The type of metal precursor is likely to be the most important cause of formation of fcc Ru. That is to say, the metal precursor that dissolves into the organic solvent as a neutral molecule rather than as an ion leads to fcc Ru. In addition, the catalytic activity for CO oxidation of the Ru nanoparticles supported on γ-Al_2O_3 was structure- and size-dependent. From the present results, other metal nanoparticles could possibly form unknown structures in the bulk state, providing unique and valuable properties that are different from those of the conventional materials.

■ ASSOCIATED CONTENT

Supporting Information

Experimental details, in situ PXRD patterns, SAED patterns and HRTEM images, and variation in CO conversion with temperature. This material is available free of charge via the Internet at http://pubs.acs.org.

■ AUTHOR INFORMATION

Corresponding Author

kitagawa@kuchem.kyoto-u.ac.jp

Notes

The authors declare no competing financial interest.

■ ACKNOWLEDGMENTS

This work was partially supported by Grants-in-Aid for the Global COE Program, Kyushu University, "Science for Future Molecular Systems"; the Elements Science and Technology Project from the MEXT, Japan; and a Research Fellowship for Young Scientists (22·3504) from JSPS.

■ REFERENCES

(1) Pettifor, D. G. *Calphad* **1977**, *1*, 305.
(2) (a) Saunders, N.; Miodownik, A. P.; Dinsdale, A. T. *Calphad* **1988**, *12*, 351. (b) Xia, H.; Parthasarathy, G.; Luo, H.; Vohra, Y. K.; Ruoff, A. L. *Phys. Rev. B* **1990**, *42*, 6736. (c) Hanfland, M.; Syassen, K.; Christensen, N. E.; Novikov, D. L. *Nature* **2000**, *408*, 174. (d) Shimizu, K.; Ishikawa, H.; Takao, D.; Yagi, T.; Amaya, K. *Nature* **2002**, *419*, 597. (e) Errandonea, D.; Meng, Y.; Häusermann, D.; Uchida, T. *J. Phys.: Condens. Matter* **2003**, *15*, 1277. (f) Ma, Y.; Eremets, M.; Oganov, A. R.; Xie, Y.; Trojan, I.; Medvedev, S.; Lyakhov, A. O.; Valle, M.; Prakapenka, V. *Nature* **2009**, *458*, 182. (g) Liu, Q.; Fan, C.; Zhang, R. *J. Appl. Phys.* **2009**, *105*, No. 123505. (h) Tateno, S.; Hirose, K.; Ohishi, Y.; Tatsumi, Y. *Science* **2010**, *330*, 359. (i) Stixrude, L. *Phys. Rev. Lett.* **2012**, *108*, No. 055505. (j) Hrubiak, R.; Drozd, V.; Karbasi, A.; Saxena, S. K. *J. Appl. Phys.* **2012**, *111*, No. 112612.

(3) (a) Xiong, S.; Qi, W.; Huang, B.; Wang, M.; Li, Z.; Liang, S. *J. Phys. Chem. C* **2012**, *116*, 237. (b) Jesser, W. A.; Shneck, R. Z.; Gile, W. W. *Phys. Rev. B* **2004**, *69*, No. 144121. (c) Calvo, F.; Doye, J. P. K. *Phys. Rev. B* **2004**, *69*, No. 125414.
(4) (a) Dong, X. L.; Choi, C. J.; Kim, B. K. *Scr. Mater.* **2002**, *47*, 857. (b) Ling, T.; Xie, L.; Zhu, J.; Yu, H.; Ye, H.; Yu, R.; Cheng, Z.; Liu, L.; Yang, G.; Cheng, Z.; Wang, Y.; Ma, X. *Nano Lett.* **2009**, *9*, 1572. (c) Kim, H.; Kaufman, M. J.; Sigmund, W. M.; Jacques, D.; Andrews, R. *J. Mater. Res.* **2003**, *18*, 1104.
(5) (a) Perkas, N.; Teo, J.; Shen, S.; Wang, Z.; Highfield, J.; Zhong, Z.; Gedaken, A. *Phys. Chem. Chem. Phys.* **2011**, *13*, 15690. (b) Carballo, J. M. G.; Yang, J.; Holmen, A.; García-Rodríguez, S.; Rojas, S.; Ojeda, M.; Fierro, J. L. G. *J. Catal.* **2011**, *284*, 102. (c) Kim, Y. H.; Yim, S.; Park, E. D. *Catal. Today* **2012**, *185*, 143. (d) Strebel, C.; Murphy, S.; Nielsen, R. M.; Nielsen, J. H.; Chorkendorff, I. *Phys. Chem. Chem. Phys.* **2012**, *14*, 8005. (e) Wendt, S.; Knapp, M.; Over, H. *J. Am. Chem. Soc.* **2004**, *126*, 1537.
(6) (a) Ertl, G. *Angew. Chem., Int. Ed.* **2008**, *47*, 3524. (b) Xie, X.; Li, Y.; Liu, Z.; Haruta, M.; Shen, W. *Nature* **2009**, *458*, 746. (c) Kaden, W. E.; Wu, T.; Kunkel, W. A.; Anderson, S. L. *Science* **2009**, *326*, 826. (d) Alayoglu, S.; Nilekar, A. U.; Mavrikakis, M.; Eichhorn, B. *Nat. Mater.* **2008**, *7*, 333. (e) Qiao, B.; Wang, A.; Yang, X.; Allard, L. F.; Jiang, Z.; Cui, Y.; Liu, J.; Li, J.; Zhang, T. *Nat. Chem.* **2011**, *3*, 634. (f) Roth, C.; Benker, N.; Buhrmester, T.; Mazurek, M.; Loster, M.; Fuess, H.; Koningsberger, D. C.; Ramaker, D. E. *J. Am. Chem. Soc.* **2005**, *127*, 14607. (g) Jiang, H.; Liu, B.; Akita, T.; Haruta, M.; Sakurai, H.; Xu, Q. *J. Am. Chem. Soc.* **2009**, *131*, 11302. (h) Kim, H. Y.; Lee, H. M.; Henkelman, G. *J. Am. Chem. Soc.* **2012**, *134*, 1560.
(7) (a) Lee, H. C.; Potapova, Y.; Lee, D. *J. Power Sources* **2012**, *216*, 256. (b) McFarland, E. *Science* **2012**, *338*, 340.
(8) (a) Kobayashi, M.; Kai, T.; Takano, N.; Shiiki, K. *J. Phys.: Condens. Matter* **1995**, *7*, 1835. (b) Watanabe, S.; Komine, T.; Kai, T.; Shiiki, K. *J. Magn. Magn. Mater.* **2000**, *220*, 277.
(9) (a) Lim, B.; Jiang, M.; Tao, J.; Camargo, P. H. C.; Zhu, Y.; Xia, Y. *Adv. Funct. Mater.* **2009**, *19*, 189. (b) Tsuji, M.; Nishizawa, Y.; Matsumoto, K.; Miyamae, N.; Tsuji, T.; Zhang, X. *Colloids Surf., A* **2007**, *293*, 185. (c) González, A. L.; Noguez, C.; Ortiz, G. P.; Rodríguez-Gattorno, G. *J. Phys. Chem. B* **2005**, *109*, 17512.
(10) (a) Grass, M. E.; Zhang, Y.; Butcher, D. R.; Park, J. Y.; Li, Y.; Bluhm, H.; Bratlie, K. M.; Zhang, T.; Somorjai, G. A. *Angew. Chem., Int. Ed.* **2008**, *47*, 8893. (b) Haruta, M.; Tsubota, S.; Kobayashi, T.; Kageyama, H.; Genet, M. J.; Delmon, B. *J. Catal.* **1993**, *144*, 175.
(11) McCarthy, E.; Zahradnik, J.; Kuczynski, G. C.; Carberry, J. J. *J. Catal.* **1975**, *39*, 29.
(12) (a) Over, H.; Kim, Y. D.; Seitsonen, A. P.; Wendt, S.; Lundgren, E.; Schmid, M.; Varga, P.; Morgante, A.; Ertl, G. *Science* **2000**, *287*, 1474. (b) Gong, X.; Liu, Z.; Raval, R.; Hu, P. *J. Am. Chem. Soc.* **2004**, *126*, 8. (c) Reuter, K.; Scheffler, M. *Phys. Rev. B* **2003**, *68*, No. 045407.
(13) Teranishi, T.; Kurita, R.; Miyake, M. *J. Inorg. Organomet. Polym.* **2000**, *10*, 145.